Ocean Systems Engineering, *Vol. 14, No. 3 (2024) 237-259*
https://doi.org/10.12989/ose.2024.14.3.237

Stress concentration factors for multi-planar tubular KK-joints of jacket substructures in offshore wind turbines

Hamid Ahmadi*[1,2] and Adel Alizadeh Atalo[3]

[1]National Centre for Maritime Engineering and Hydrodynamics, Australian Maritime College, University of Tasmania, Australia
[2]Centre for Future Materials, Institute for Advanced Engineering and Space Sciences, University of Southern Queensland, Australia
[3]Faculty of Civil Engineering, University of Tabriz, Iran

(Received May 23, 2024, Revised August 17, 2024, Accepted September 10, 2024)

Abstract. Although the investigation on the effect of loaded out-of-plane braces on the values of the stress concentration factor (SCF) in offshore tubular joints has been the objective of numerous research works, a number of quite important cases still exist that have not been studied thoroughly due to the diversity of joint types and loading conditions. One of these cases is the multi-planar tubular KK-joint subjected to axial loading. Tubular KK-joints are among the most common joint types in jacket substructure of offshore wind turbines (OWTs). In the present research, data extracted from the stress analysis of 243 finite element (FE) models, verified against available experimental data, was used to study the effects of geometrical parameters on the chord-side SCFs in multi-planar tubular KK-joints subjected to axial loading. Parametric FE study was followed by a set of nonlinear regression analyses to develop three new SCF parametric equations for the fatigue analysis and design of axially loaded multi-planar KK-joints.

Keywords: fatigue; jacket substructure; offshore wind turbine (OWT); multi-planar tubular KK-joint; stress concentration factor (SCF)

1. Introduction

The primary structural part of a jacket-type offshore wind turbine (OWT), i.e., the jacket substructure (Fig. 1(a)), is fabricated from tubular members by welding one end of the branch members, i.e., braces, to the undisturbed surface of the main member, i.e., chord, resulting in what is known as a tubular joint (Fig. 1(b)). As a result of the formation and propagation of cracks due to wave induced cyclic loads, tubular joints are susceptible to fatigue-induced damage during their service life.

The significant stress concentrations at the vicinity of the welds are considerably detrimental to the fatigue performance of the joints. Hence, it is important to accurately determine the magnitude of stress concentration and to reduce it to a reasonable level. In the design practice, a parameter called the stress concentration factor (SCF) is used to evaluate the magnitude of the stress concentration. The SCF, defined as the ratio of the local surface stress at the brace-to-chord

*Corresponding author, Dr., E-mail: hamid.ahmadi@utas.edu.au

http://www.techno-press.org/?journal=ose&subpage=7 ISSN: 2093-6702 (Print), 2093-677X (Online)

intersection to the nominal stress in the brace, exhibits considerable scatter depending on the joint geometry, loading type, weld size and type, and the considered position for the SCF calculation around the weld profile.

The SCF value along the weld toe of a tubular joint under any specific loading condition is mainly determined by the joint geometry. To study the behavior of tubular joints and to easily relate this behavior to the geometrical characteristics of the joint, a set of dimensionless geometrical parameters has been defined. Fig. 1(b) depicts a multi-planar tubular KK-joint, also called a two-planar K-joint or a DK-joint, with the geometrical parameters τ, γ, β, θ, ζ, α, and α_B for chord and brace diameters D and d, their corresponding wall thicknesses T and t, and respective lengths L and l. Critical positions along the weld toe of the brace-to-chord intersection for the calculation of the SCF values in a tubular DK-joint, i.e., inner saddle, outer saddle, toe, and heel are shown in Fig. 1(b).

Significant effort has been devoted, over the past five decades, to the study of SCFs in various uniplanar tubular joints (i.e., joints where the axes of the chord and brace members lay on the same plane). As a result, many parametric design formulas in terms of the joint's geometrical parameters have been proposed providing SCF values at certain positions adjacent to the weld for several loading conditions. Multi-planar joints (i.e., joints where the axes of the chord and all brace members do not lay on the same plane) are an intrinsic feature of offshore tubular structures. The multi-planarity effect might play an important role in the stress distribution along the brace-to-chord intersection. Thus, for multi-planar connections, the parametric formulae of simple uniplanar tubular joints may not be applicable for the SCF prediction; since such formulae may lead to highly over- or under-predicting results. Nevertheless, for multi-planar joints covering the majority of practical applications, fewer investigations have been reported due to the complexity and high cost involved. Results of a numerical study on the SCFs in multi-planar tubular KK-joints are discussed in the present paper. In this research program, a set of parametric finite element (FE) stress analyses was carried out on 243 tubular DK-joint models subjected to axial loading (Fig. 1(c)). Analysis results were used to present general remarks on the effects of geometrical parameters including τ (brace-to-chord thickness ratio), γ (chord wall slenderness ratio), β (brace-to-chord diameter ratio), θ (brace inclination angle), and ζ (relative gap) on the SCF values at the inner saddle, outer saddle, toe, and heel positions. Based on the results of DK-joint FE models, verified using available experimental data, a SCF database was prepared. Then, a new set of SCF parametric equations was established, based on nonlinear regression analyses, for the fatigue analysis and design of multi-planar tubular KK-joints subjected to axial loading. The reliability of proposed equations was evaluated according to the acceptance criteria recommended by the UK Department of Energy (DoE) (1983).

2. Literature review

2.1 SCF calculation for uniplanar tubular joints

For investigating the SCFs in unstiffened uniplanar tubular joints, the reader is referred to Kuang *et al*. (1975), Efthymiou (1988), Hellier *et al.* (1990), UK HSE OTH 354 (1997), and Karamanos *et al.* (2000) for the SCF calculation at the saddle and crown positions of simple uniplanar T-, Y-, X-, K-, and KT-joints; and Gho and Gao (2004), Gao (2006), Gao *et al*. (2007), and Yang *et al.* (2015) for the SCF determination in overlapped uniplanar joints, among others.

For the study of SCF distribution along the weld toe in unstiffened uniplanar tubular joints, the reader is referred for example to Morgan and Lee (1998a, b) for K-joints; Chang and Dover (1999a,

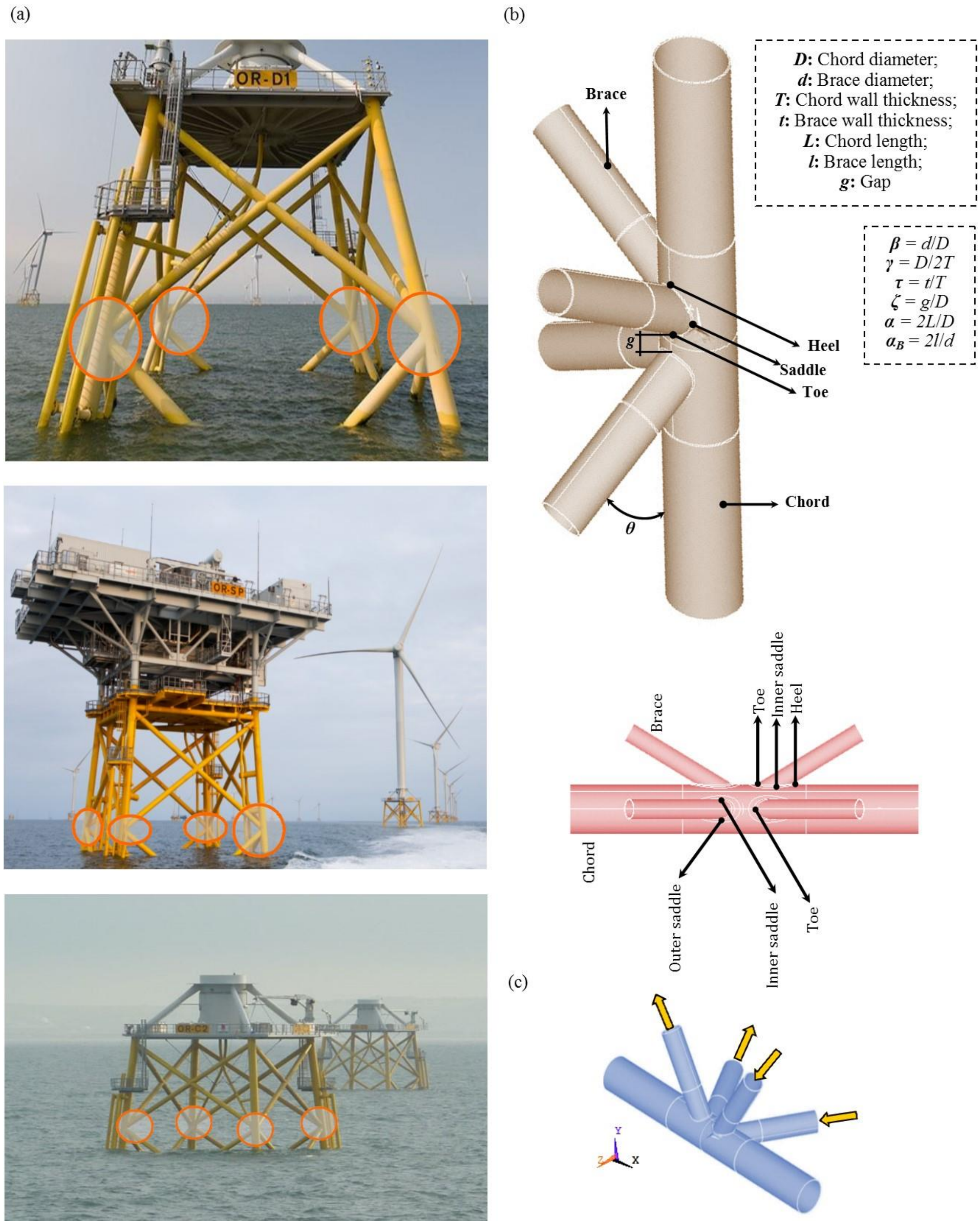

Fig. 1 (a) Multi-planar tubular KK-joints in OWT jacket substructures, (b) Geometrical notation for a multi-planar KK-joint and (c) Studied axial loading condition

b) for T-, Y-, X-, and DT-joints; Shao (2004b, 2007) and Shao *et al*. (2009) for T- and K-joints; Lotfollahi-Yaghin and Ahmadi (2010), Ahmadi et al. (2011c), and Lotfollahi-Yaghin and Ahmadi (2011) for KT- and DKT-joints; and Liu *et al.* (2015) for T-joints.

For the SCF calculation at saddle and crown positions of stiffened tubular joints, the reader is referred for example to Nwosu *et al.* (1995) for ring-stiffened T-joints; Hoon *et al*. (2001) for doubler-plate reinforced T-joints; Myers *et al*. (2001) for rack-plate reinforced joints; Ahmadi and Lotfollahi-Yaghin (2015) and Ahmadi and Zavvar (2015) for ring-stiffened KT-joints subjected to in-plane bending (IPB) moment and OPB moment loadings; and Xu *et al*. (2015) for concrete-filled joints.

Ahmadi *et al.* (2012b, 2013) investigated the SCF distribution along the weld toe of central and outer braces in tubular KT-joints reinforced with internal ring stiffeners and proposed a set of parametric equations to calculate the SCFs along the brace-to-chord intersection in internally ring-stiffened KT-joints subjected to axial loading. Nassiraei and Rezadoost (2020, 2021a, b) studied the SCFs in tubular T/Y-joints reinforced with fiber composites subjected to axial, IPB, and OPB loadings.

2.2 SCF calculation for multi-planar tubular joints

For the SCF studies in unstiffened multi-planar joints, the reader is referred to Karamanos *et al*. (1999) and Chiew *et al.* (2000) for the SCF calculation in XX-joints; Wingerde et al. (2001) for the SCF determination in KK-joints; Karamanos et al. (2002) for the study of SCFs in DT-joints; Chiew *et al*. (1999) for the study of SCFs in XT-joints; Ahmadi *et al*. (2011a, 2012a), Ahmadi and Lotfollahi-Yaghin (2012b), and Ahmadi and Zavvar (2016) for the investigation of SCFs in multi-planar KT-joints under axial loads; and Ahmadi and Kouhi (2020) for the SCF determination in unreinforced XT-joints subjected to out-of-plane bending (OPB) moment loadings, among others.

For the study of SCFs in stiffened multi-planar joints, the reader is referred to Woghiren and Brennan (2009) and Ahmadi and Imani (2022). Woghiren and Brennan (2009) developed a set of parametric equations to predict the SCFs at critical positions along the brace-chord intersection in two-planar tubular KK-joints reinforced with rack plates. Ahmadi and Imani (2022) investigated the SCFs in offshore two-planar tubular TT-joints reinforced with internal ring stiffeners.

2.3 Other studies on tubular joints

For other SCF-related research works such as probabilistic and reliability studies, the reader is referred for example to Ahmadi *et al*. (2011b), Gaspar *et al.* (2011), Ahmadi and Lotfollahi-Yaghin (2012a, 2013), Asgarian *et al.* (2014), Ahmadi and Ghaffari (2015), Ahmadi *et al.* (2015, 2016), Ahmadi (2016), Ahmadi and Mousavi Nejad Benam (2017), and Prashob et al. (2018). Regarding the local joint flexibility of tubular joints, extensive studies have been conducted by Nassiraei and Chavoshi (2024), Nassiraei (2019a, 2020, 2022), and Nassiraei and Yara (2022a, b, 2023), among others. Nassiraei (2019b, 2023, 2024a, b) investigated the strength of tubular T/Y- and X-joints reinforced with stiffener plates at ambient and elevated temperatures.

2.4 Remarks

It can be clearly concluded from Sect. 2.1–2.3 that over the past fifty years, significant effort has been devoted to the study of SCFs in various uniplanar joints. However, the study of SCFs in multi-planar joints is rather limited. Despite the frequent use of multi-planar tubular KK-joints for the fabrication of the jacket substructures in OWTs, the SCFs in axially loaded DK-joints have not been investigated and no design equation is currently available to determine the weld-toe SCFs at the saddle, toe, and heel positions in tubular DK-joints subjected to axial loading.

3. FE modeling and SCF extraction

In the present research, FE-based software package ANSYS was used for the modeling and analysis of multi-planar tubular KK-joints subjected to axial loading in order to extract the SCF values for the parametric study and formulation. This section presents the details of FE modeling and analysis.

3.1 Weld profile

One of the most critical factors affecting the accuracy of SCF results is the accurate modeling of the weld profile. Therefore, the weld sizes must be carefully included in the FE modeling. A number of research works has been carried out on the study of the weld effect. For example, the reader is referred to Lee and Wilmshurst (1995), Cao *et al*. (1997), and Lee (1999), among others. It was found that the fatigue strength of the joint can be underestimated by 20% compared to the experimental data without considering the weld (Shao 2004a).

In the present research, the welding size along the brace-to-chord intersection satisfies the AWS D 1.1 (2002) specifications. The weld sizes at the saddle, toe, and heel positions can be determined as follows

$$H_w(\text{mm}) = 0.85t(\text{mm}) + 4.24$$

$$L_w = \frac{t}{2}\left[\frac{135^\circ - \psi \text{ (deg.)}}{45^\circ}\right]$$

$$\psi = \begin{cases} 180^\circ - \left[\cos^{-1}\beta \text{ (deg.)}\right] & \text{Saddle} \\ 180^\circ - \theta \text{ (deg.)} & \text{Toe} \\ \theta \text{ (deg.)} & \text{Heel} \end{cases} \tag{1}$$

The parameters used in Eq. (1) are defined in Fig. 2. The dihedral angle (ψ) which is an important parameter in determining the weld thickness is defined as the angle between the chord and brace surface along the intersection curve.

As an example, the weld profile generated for a sample joint model ($\beta = 0.4$, $\gamma = 12$, $\tau = 0.7$, $\theta = 45^\circ$) is shown in Fig. 3. For details of the weld profile modeling according to AWS D 1.1 (2002) specifications, the reader is referred to Ahmadi *et al.* (2012a). It should be noted that attempts to produce an improved as-welded profile often result in over-welding. Consequently, the actual weld size, typical of yard practice, is usually different from the nominal weld size recommended by AWS D 1.1 (2002). For the correction of SCFs to consider the actual position of the weld toe, the reader is advised to follow the recommendations of Section C 5.3.2(a) of API RP 2A (2007).

Considering the effect of possible weld defects, the hot-spot stress (HSS) method has been quite efficient and popular for fatigue design purposes. According to this method, the nominal stress at

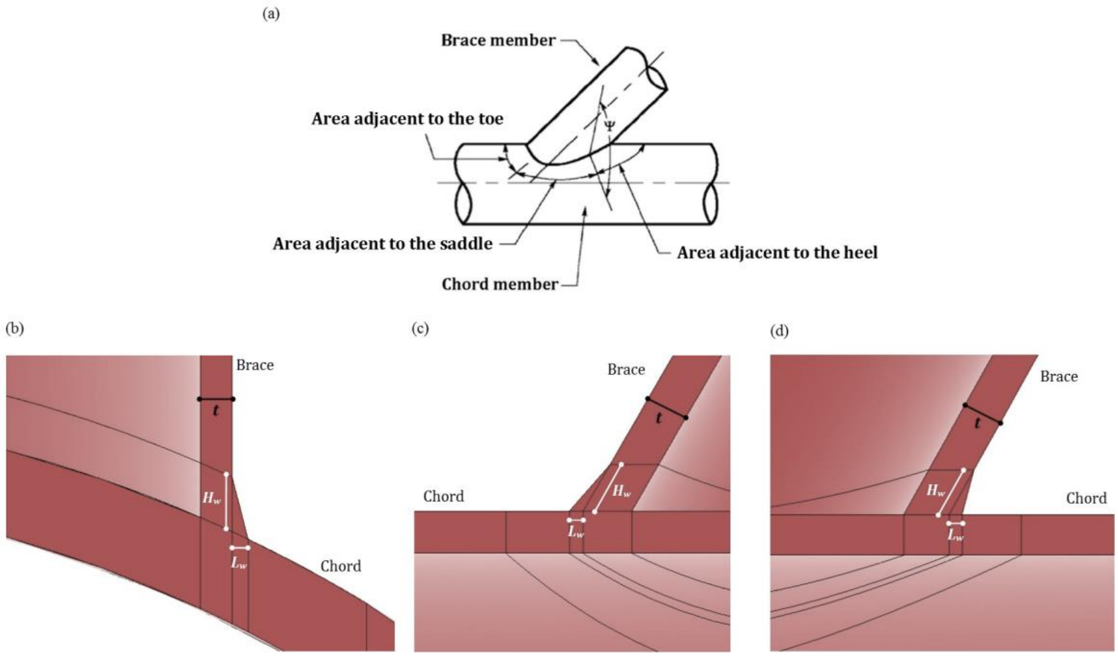

Fig. 2(a) Definition of the dihedral angle, (b) weld dimensions at the saddle position, (c) weld dimensions at the toe position and (d) weld dimensions at the heel position

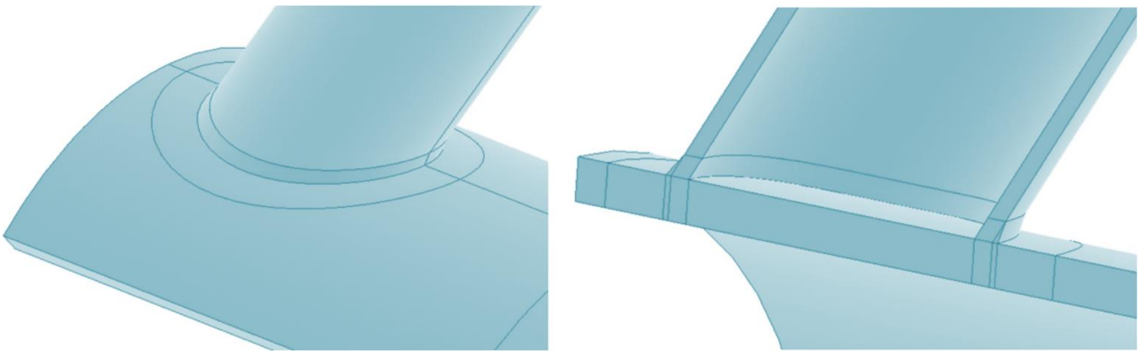

Fig. 3 The weld profile generated for a sample joint model ($\beta = 0.4$, $\gamma = 12$, $\tau = 0.7$, $\theta = 45^{\circ}$)

the joint members is multiplied by an appropriate SCF to provide the HSS at a certain location. HSSs are calculated at various positions around the weld and the maximum HSS range (S) is determined. Then, the fatigue life of the joint is estimated through an appropriate S–N fatigue curve, N being the number of load cycles. The HSS range concept places different structural geometries on a common basis, enabling them to be treated using a single S–N curve. The basis of this concept is to capture a stress (or strain) in the proximity of the weld toes, which characterizes the fatigue life of the joint, but excludes the very local microscopic effects like the sharp notch, undercut and crack-like defects at the weld toe. These local weld notch effects are included in the S–N curve.

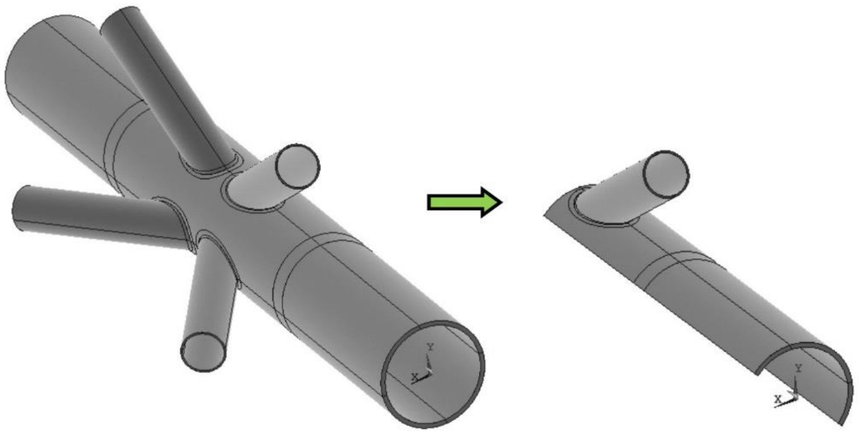

Fig. 4 One quarter of the entire multi-planar tubular KK-joint required to be modeled under studied axial loading condition

3.2 Boundary conditions

The chord end fixity conditions of tubular joints in offshore structures may range from almost fixed to almost pinned with generally being closer to almost fixed (Efthymiou 1988). In practice, the value of the parameter α in over 60% of tubular joints is in excess of 20 and is bigger than 40 in 35% of the joints (Smedley and Fisher 1991). Changing the end restraint from fixed to pinned results in a maximum increase of 15% in the SCF at the crown position for joints with $\alpha = 6$, and this increase reduces to only 8% for $\alpha = 8$ (Morgan and Lee 1998b). In the view of the fact that the effect of chord end restraints is only significant for joints with $\alpha < 8$ and high β and γ values, which do not commonly occur in practice, both chord ends were assumed to be fixed, with the corresponding nodes restrained.

Due to the symmetry in geometry and loading of the joint, only ¼ of the entire multi-planar tubular KK-joint is required to be modeled in order to reduce the computational time (Fig. 4).

3.3 Mesh generation

ANSYS element SOLID95 was used in the present study to model the chord, braces, and weld profiles. This element type has compatible displacements and is well-suited to model curved boundaries. It is defined by 20 nodes having three degrees of freedom per node and may have any spatial orientation. Using this type of 3-D brick elements, the weld profile can be modeled as a sharp notch. This method will produce more accurate and detailed stress distribution near the intersection in comparison with a shell analysis.

A sub-zone mesh generation scheme was used during the FE modeling in order to guarantee the mesh quality. The entire structure was divided to several zones according to computational requirements. The mesh of each zone was generated separately and then the mesh of the entire joint was produced by merging the meshes of all the sub-zones. This scheme can feasibly control the mesh quantity and quality and avoid badly distorted elements. The mesh generated by this procedure for a multi-planar tubular KK-joint is shown in Fig. 5(a).

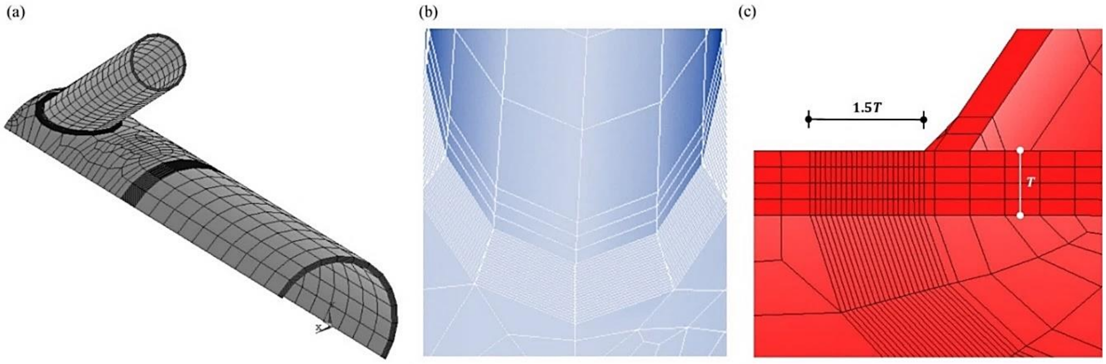

Fig. 5 Generated mesh by the sub-zone scheme: (a) One quarter of the joint under the axial loading condition, (b) Weld profile and extrapolation region and (c) Regions adjacent to the brace-to-chord intersection

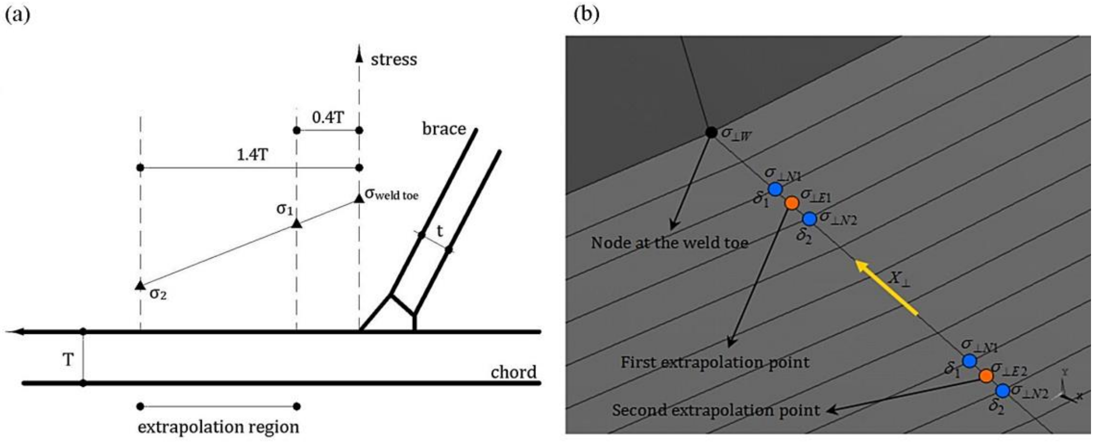

Fig. 6 (a) Extrapolation method according to IIW XV-E (1999) and (b) Required interpolations and extrapolations to extract the HSS value at the weld toe

As mentioned earlier, in order to determine the SCF, the stress at the weld toe should be divided by the nominal stress of the loaded brace. The stresses perpendicular to the weld toe at the extrapolation points are required to be calculated in order to determine the stress at the weld toe position. To extract and extrapolate the stresses perpendicular to the weld toe, as shown in Figs. 5(b) and 6(b), the region between the weld toe and the second extrapolation point was meshed finely in such a way that each extrapolation point was placed between two nodes located in its immediate vicinity. These nodes are located on the element-generated paths which are perpendicular to the weld toe.

In order to make sure that the results of the FE analysis are not affected by the inadequate quality or the size of the generated mesh, convergence test was conducted and meshes with different densities were used in this test, before generating the 243 models. Based on the results of convergence test, the number of elements through the chord and brace thickness was 4 and 1, respectively (Fig. 5(c)); the number of elements on the surface, base, and back of the weld profile was 3, 1, and 2, respectively (Figs. 5(b) and 5(c)); the number of elements along a full brace-to-chord intersection was selected to be 16 (Fig. 5(a)); and the number of elements inside the extrapolation region was selected to be 22 (Fig. 5(c)).

3.4 Analysis and SCF determination

Static analysis of the linearly elastic type is suitable to determine the SCFs in tubular joints (N'Diaye *et al*. 2007). The Young's modulus and Poisson's ratio were taken to be 207 GPa and 0.3, respectively.

The weld-toe SCF is defined as

$$\mathrm{SCF} = \sigma_{\perp W} / \sigma_n \tag{2}$$

In Eq. (2), σ_n is the nominal stress of the axially loaded brace which is calculated as follows

$$\sigma_n = \frac{4F_a}{\pi\left[d^2 - (d-2t)^2\right]} \tag{3}$$

where F_a is the applied axial force; and d and t are brace diameter and thickness, respectively.

To calculate the SCF, the stress at the weld toe position should be extracted from the stress field outside the region influenced by the local weld toe geometry. The location from which the stresses have to be extrapolated, *extrapolation region*, depends on the dimensions of the joint and on the position along the intersection. According to the linear extrapolation method recommended by IIW XV-E (1999), the first extrapolation point must be at a distance of $0.4T$ from the weld toe, and the second point should lie at $1.0T$ further from the first point (Fig. 6(a)). In Eq. (2), $\sigma_{\perp W}$ is the extrapolated stress at the weld toe position which is perpendicular to the weld toe and is calculated by the following equation

$$\sigma_{\perp W} = 1.4\sigma_{\perp E1} - 0.4\sigma_{\perp E2} \tag{4}$$

where $\sigma_{\perp E1}$ and $\sigma_{\perp E2}$ are the stresses at the first and second extrapolation points along the direction perpendicular to the weld toe, respectively.

The stress at an extrapolation point is obtained as follows

$$\sigma_{\perp E} = \frac{\sigma_{\perp N1} - \sigma_{\perp N2}}{\delta_1 - \delta_2}\left(\Delta - \delta_2\right) + \sigma_{\perp N2} \tag{5}$$

where $\sigma_{\perp Ni}$ (i = 1 and 2) is the nodal stress at the immediate vicinity of the extrapolation point along the direction perpendicular to the weld toe at the saddle position (Eq. (6)); δ_i (i = 1 and 2) is the distance between the weld toe and the considered node inside the extrapolation region (Eq. (7)); and Δ equals to $0.4T$ and $1.4T$ for the first and second extrapolation points, respectively (Fig. 6(b)).

$$\sigma_{\perp N} = \sigma_x l_1^2 + \sigma_y m_1^2 + \sigma_z n_1^2 + 2\left(\tau_{xy} l_1 m_1 + \tau_{yz} m_1 n_1 + \tau_{zx} n_1 l_1\right) \tag{6}$$

$$\delta = \sqrt{\left(x_w - x_n\right)^2 + \left(y_w - y_n\right)^2 + \left(z_w - z_n\right)^2} \tag{7}$$

Table 1 Properties of uniplanar tubular K-joint used for the verification of present FE model

Joint ID (HSE OTH 354 1997)	Material	Loading type	D (mm)	τ	β	γ	α	ζ	θ
K-4	Steel	Axial	216	0.88	0.28	13.5	10.2	0.11	60°

Table 2 Results of the FE model verification based on HSE OTH 354 (1997) experimental data

Position	SCF		Difference
	Present FE model	Experimental data (HSE OTH 354 1997)	
Saddle	4.12	3.60	14.44%
Toe	4.67	5.40	13.51%

In Eq. (6), σ_a and τ_{ab} (a, b = x, y, z) are components of the stress tensor which can be extracted from ANSYS analysis results; and l_1, m_1, and n_1 are transformation components defined as

$$l_1 = \cos\left(X_\perp, x\right); \quad m_1 = \cos\left(X_\perp, y\right); \quad n_1 = \cos\left(X_\perp, z\right) \tag{8}$$

where $X_\perp$ is the direction perpendicular to the weld toe; and x, y, and z are axes of the global coordinate system (Fig. 6b). These components can be calculated as below

$$l_1 = \left(x_w - x_n\right)/\delta; \quad m_1 = \left(y_w - y_n\right)/\delta; \quad n_1 = \left(z_w - z_n\right)/\delta \tag{9}$$

where (x_n , y_n , z_n) and (x_w , y_w , z_w) are global coordinates of the considered node inside the extrapolation region and its corresponding node at the weld toe position, respectively.

At the saddle, toe, and heel positions, Eq. (6) is simplified as

$$\sigma_{\perp N} = \sigma_y m_1^2 + \sigma_z n_1^2 + 2\tau_{yz} m_1 n_1 \ \text{(Saddle)}; \quad \sigma_{\perp N} = \sigma_x \ \text{(Toe and Heel)} \tag{10}$$

In order to facilitate the SCF calculation, above formulation was implemented in a *macro* developed by the ANSYS Parametric Design Language (APDL). The input data required to be provided by the user of the macro are the node number at the weld toe, the chord thickness, and the numbers of the nodes inside the extrapolation region. These nodes can be introduced using the Graphic user interface (GUI).

3.5 FE model verification

As far the authors are aware, there is no experimental/numerical data available in the literature on the SCFs in axially loaded multi-planar tubular KK-joints that are studied in the present research. However, a set of related experimental data is available that can be used to verify the present FE models.

To validate the present FE models, experimental data on the SCFs of uniplanar K-joints published in HSE OTH 354 (1997) was used. In order to do so, an FE model was generated for a K-joint having the same geometrical characteristics as the K-4 specimen (Table 1) and the model was analyzed subjected to the brace axial loading (Fig. 7). The method of geometrical modeling (introducing the

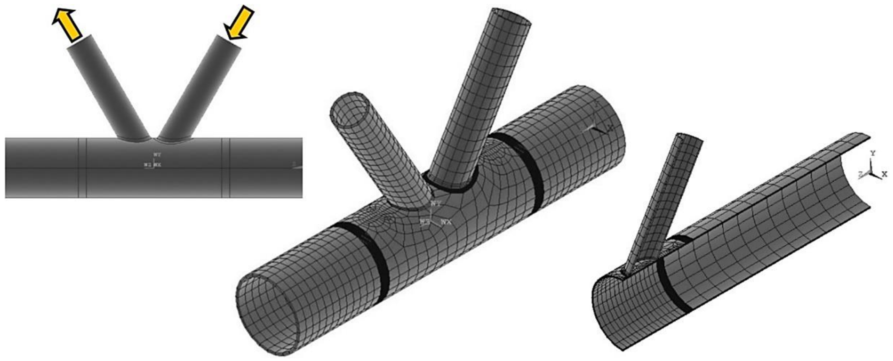

Fig. 7 Validating FE model generated for the comparison of the results with HSE OTH 354 (1997) experimental measurements

Table 3 Values assigned to each dimensionless parameter

Parameter	Definition	Value(s)
β	d/D	0.3, 0.4, 0.5
γ	$D/2T$	12, 18, 24
τ	t/T	0.4, 0.7, 1.0
ζ	g/D	0.2, 0.4, 0.6
θ	Brace inclination angle	30°, 45°, 60°
α	$2L/D$	16
α_B	$2l/d$	8

chord, brace, and weld profile), the mesh generation procedure (including the selection of element type and size), load application, analysis method, and the method of SCF extraction are identical for the K-joint validating model and the DK-joint models used for the parametric study. Hence, the verification of SCF values derived from validating FE model with the experimental data from HSE OTH 354 (1997) lends some support to the validity of SCF values derived from the FE models of present paper. Result of verification process presented in Table 2 shows that the maximum difference between the numerical and experimental results is less than 15% indicating that there is a good agreement between the results of present FE model and HSE OTH 354 (1997) experimental data. Hence, generated FE models can be considered to be accurate enough to provide valid results.

4. Geometrical effects on the SCFs

4.1 Settings of parametric study

To study the SCFs in multi-planar KK-joints subjected to axial loading (Fig. 1(c)), 243 models were generated and analyzed using the FE software, ANSYS. The objective was to investigate the effects of non-dimensional geometrical parameters on the chord-side SCFs at the inner saddle, outer saddle, toe, and heel positions.

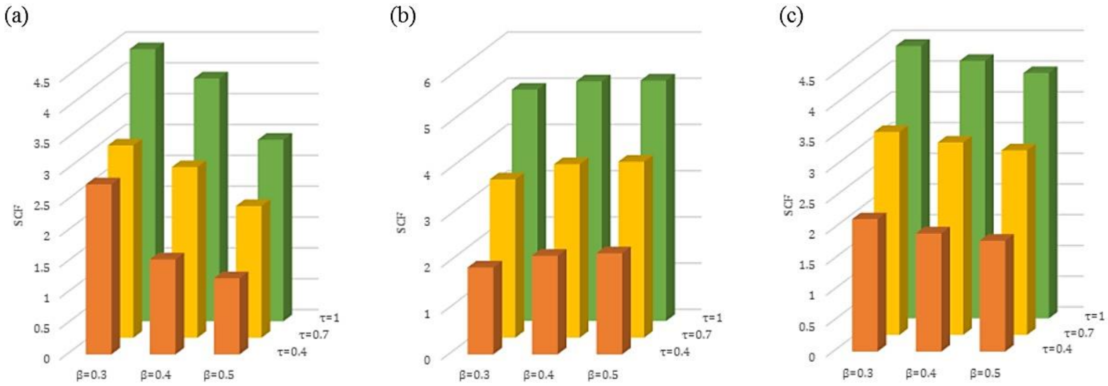

Fig. 8 The effect of the β on the SCF values and its interaction with the τ ($\theta = 60^{\circ}$, $\zeta = 0.2$, $\gamma = 12$): (a) Inner saddle position, (b) Outer saddle position and (c) Toe position

Different values assigned to parameters β, γ, τ, ζ, and θ have been presented in Table 3. These values cover the practical ranges of dimensionless parameters typically found in tubular joints of OWT jacket substructures. Sufficiently long chord greater than six chord diameters (i.e., $\alpha \geq 12$) should be used to ensure that the stresses at the brace-to-chord intersection are not affected by the chord's boundary conditions (Efthymiou 1988). Hence, in this study, a realistic value of $\alpha = 16$ was designated for all the models. The brace length has no effect on the HSSs when the parameter α_B is greater than a critical value (Chang and Dover 1999a). According to Chang and Dover (1996), this critical value is about 6. In the present study, in order to avoid the effect of short brace length, a realistic value of $\alpha_B = 8$ was assigned to all joints. The 243 generated models span the following ranges of dimensionless geometrical parameters

$$\begin{gathered} 0.3 \leq \beta \leq 0.5 \\ 12 \leq \gamma \leq 24 \\ 0.4 \leq \tau \leq 1.0 \\ 0.2 \leq \zeta \leq 0.6 \\ 30^{\circ} \leq \theta \leq 60^{\circ} \end{gathered} \tag{11}$$

4.2 Effects of the β, τ, γ, ζ, and θ

Since the parameter β is the ratio of brace diameter to chord diameter, the increase of the β in models having constant value of chord diameter results in the increase of brace diameter. Three charts are given in Fig. 8, as an example, depicting the change of the SCF values at the inner saddle (IS), outer saddle (OS), and toe (T) positions due to the change in the value of the β and the interaction of this parameter with the τ. The IS, OS, and T positions are shown in Fig. 1(b). In this study, the influence of parameters γ, ζ, and θ over the effect of the β on the SCF was also investigated. A large number of comparative charts were used to study the effect of the β and only three of them are presented here for the sake of brevity. Results showed that the increase of the β generally results in the decrease of the SCF values at the IS and T positions and a slight increase of SCFs at the OS position which is negligible.

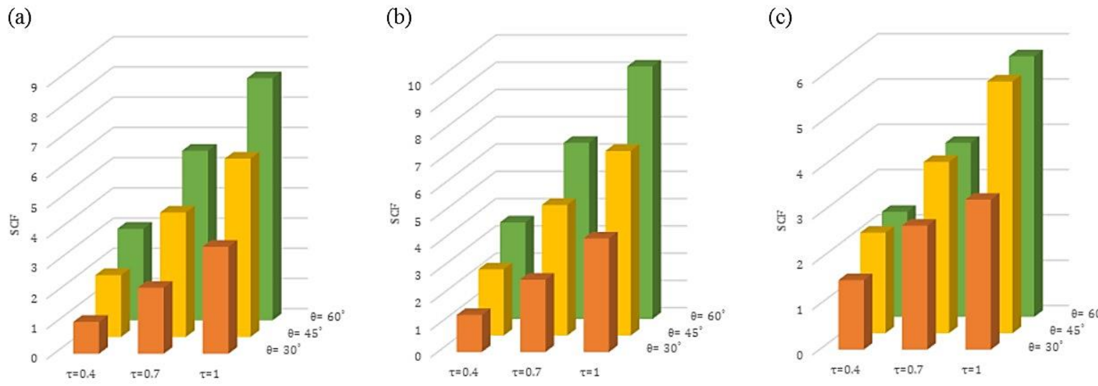

Fig. 9 The effect of the τ on the SCF values and its interaction with the θ (β = 0.3, ζ = 0.4, γ = 18): (a) Inner saddle position, (b) Outer saddle position and (c) Toe position

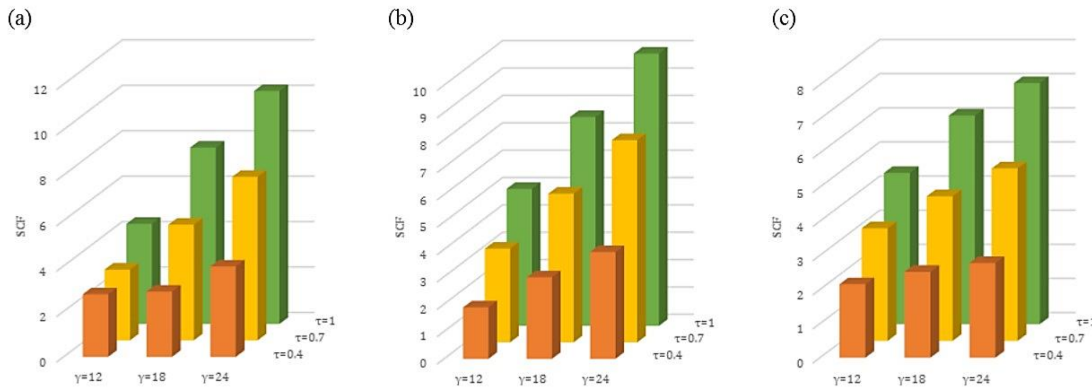

Fig. 10 The effect of the γ on the SCF values and its interaction with the τ (θ = 60°, ζ = 0.2, β = 0.3): (a) Inner saddle position, (b) Outer saddle position and (c) Toe position

Since the parameter τ is the ratio of brace thickness to chord thickness and the γ is the ratio of radius to thickness of the chord, the increase of the τ in models having constant value of the γ results in the increase of the brace thickness. For example, Fig. 9 shows the change of the SCF values at the IS, OS, and T positions due to the change in the value of the τ and the interaction of this parameter with the γ. In this study, the interaction of the τ with the other geometrical parameters was also investigated. Results indicated that the increase of the τ leads to the increase of the SCF at the IS, OS, and T positions. This conclusion is independent from the values of other geometrical parameters.

Since the parameter γ is the ratio of the radius to the thickness of the chord, the increase of the γ in models having constant value of the chord diameter means the decrease of chord thickness. Three charts are presented in Fig. 10, as an example, depicting the change of the SCF at the IS, OS, and T positions due to the change in the value of the γ and the interaction of this parameter with the τ. In this study, the influence of parameters β, ζ, and θ over the effect of the γ on SCF values was also investigated. It was observed that the increase of the γ leads to the increase of the SCF at the IS, OS, and T positions. This behavior does not depend on the values of other geometrical parameters.

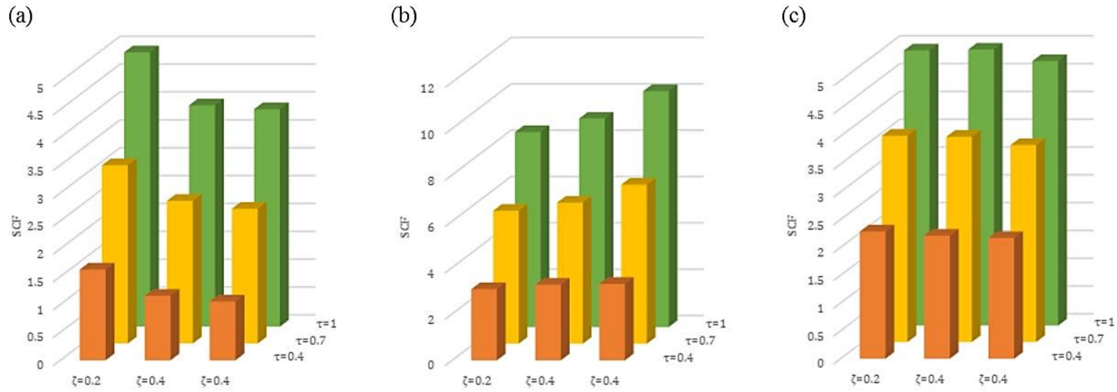

Fig. 11 The effect of the ζ on the SCF values and its interaction with the τ ($\theta = 45^{\circ}$, $\gamma = 24$, $\beta = 0.5$): (a) Inner saddle position, (b) Outer saddle position and (c) Toe position

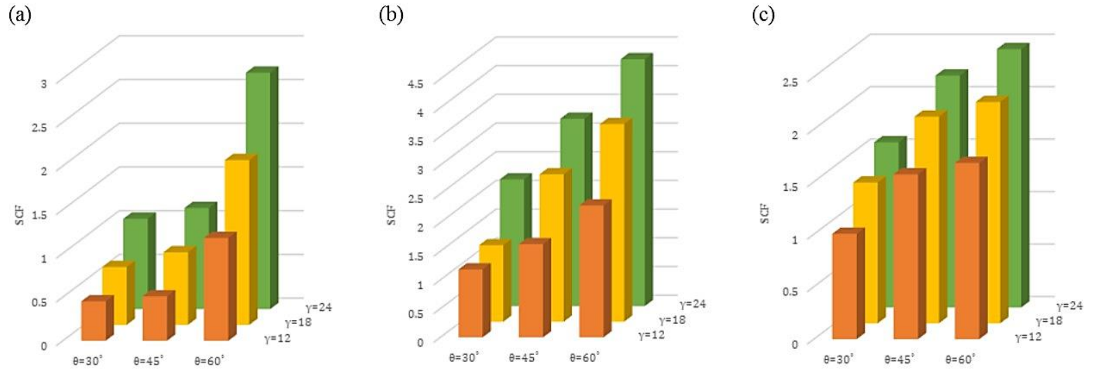

Fig. 12 The effect of the θ on the SCF values and its interaction with the γ ($\zeta = 0.4$, $\beta = 0.5$, $\tau = 0.4$): (a) Inner saddle position, (b) Outer saddle position and (c) Toe position

Since the parameter ζ is the ratio of the gap (defined in Fig. 1(b)) to the chord diameter, the increase of the ζ in models having constant value of the chord diameter means the increase of the gap. For example, Fig. 11 shows the change of the SCF values at the IS, OS, and T positions due to the change in the value of the ζ and the interaction of this parameter with the τ. In this study, the interaction of the ζ with the other geometrical parameters was also investigated. Results showed that the increase of the ζ generally leads to the decrease of the SCFs at the IS and T positions, while its increase results in the increase of the SCF values at the OS position. It should be noted that the effect of the ζ on the SCF values is more highlighted at the IS position compared to the OS and T positions. The reason behind the decrease of the SCFs at the IS position due the increase of the ζ is that the increase of the ζ leads to the decrease of the local deformation of the chord at the IS position implying that the increase of the ζ results in the increase of the local stiffness of the joint at the IS position which consequently leads to the decrease of the SCF at this position.

The parameter θ is the brace inclination angle shown in Fig. 1(b). Three charts are presented in Fig. 12, as an example, depicting the change of the SCF at the IS, OS, and T positions due to the

Table 4 Comparison of SCF values at different positions in nine sample multi-planar KK-joints subject to axial loading

Joint ID	Geometrical properties								SCF			
	D (mm)	τ	β	γ	ζ	θ	α	α_B	Inner saddle	Outer saddle	Toe	Heel
DK235	500	1	0.5	12	0.2	60˚	16	8	2.9422	4.9923	3.9934	1.3367
DK236	500	1	0.5	18	0.2	60˚	16	8	4.8367	7.5951	5.2567	2.1908
DK237	500	1	0.5	24	0.2	60˚	16	8	6.7649	9.9128	6.1181	2.6737
DK238	500	1	0.5	12	0.4	60˚	16	8	2.8559	5.5545	3.6822	1.4618
DK239	500	1	0.5	18	0.4	60˚	16	8	4.7039	8.7836	4.8381	2.1710
DK240	500	1	0.5	24	0.4	60˚	16	8	6.8963	11.2421	5.7410	2.7463
DK241	500	1	0.5	12	0.6	60˚	16	8	2.8001	5.8522	3.7019	1.5379
DK242	500	1	0.5	18	0.6	60˚	16	8	4.6033	9.2249	4.6901	2.1855
DK243	500	1	0.5	24	0.6	60˚	16	8	6.4831	12.4524	5.5461	2.7459

change in the value of the θ and the interaction of this parameter with the τ. In this study, the influence of parameters β, γ, and ζ over the effect of the θ on SCF values was also investigated. It was observed that the increase of the θ leads to the increase of the SCF at the IS, OS, and T positions.

4.3 Remarks on the biggest and smallest SCF values

By comparing the SCFs at the considered positions (Table 4), it can be concluded that:

$$SCF_{OS} > SCF_{T} > SCF_{IS} > SCF_{H} \tag{12}$$

It should be noted that the values of the SCF at the heel position are not included in Figs. 8-12. The reason is that the SCF values at this position are always quite small and even less than the unity in a large number of the FE joint models (Table 4). However, a limit on minimum SCF is necessary for conservative design of tubular joints under fatigue loading. A limit of SCF = 1.5 was previously recommended for simple tubular joints by API RP 2A (2007), UEG (1985), Smedley and Fisher (1991), and Chang and Dover (1999b). A minimum SCF value of 2.0 was recommended in CIDECT Design Guide No. 8 (2000). Efthymiou and Durkin (1985) proposed that the limit of minimum SCF for overlapped joints could be lowered to 1.0 for the chord-side SCFs. In the present study, following the CIDECT Design Guide No. 8 (2000) recommendations, a minimum value of 2.0 is proposed for the weld-toe SCFs at the heel position.

5. Deriving parametric equations for the SCF calculation

In the present paper, three individual parametric equations are proposed for the calculation of the SCF values at the inner saddle, outer saddle, and toe positions on the weld toe of multi-planar tubular KK-joints subjected to axial loading. Results of multiple nonlinear regression analyses performed by SPSS were used to develop these parametric SCF formulae. Values of dependent variable (i.e., SCF) and independent variables (i.e., β, γ, τ, ζ, and θ) constitute the input data imported in the form of a matrix. Each row of this matrix involves the information about the SCF value at a considered position on the weld toe of a multi-planar tubular KK-joint having specific geometrical properties.

When the dependent and independent variables are defined, a model expression must be built with defined parameters. Parameters of the model expression are unknown coefficients and exponents. The researcher must specify a starting value for each parameter, preferably as close as possible to the expected final solution. Various model expressions must be built to derive a parametric equation having a high coefficient of determination (R^2).

Following parametric equations are proposed, after performing a large number of nonlinear analyses, for the calculation of the SCF values at the inner saddle, outer saddle, and toe positions in tubular DK-joints subjected to axial loading condition (Fig. 1(c)):

- *Inner saddle position*

$$\mathrm{SCF_{IS}} = 2.236\beta^{1.197}\gamma^{1.275}\tau^{1.002}\zeta^{0.213}\theta^{1.189}\left(1 - 1.510\beta^{0.925} + \frac{0.125}{\tau^{0.271}\,\zeta^{0.710}}\right) \quad R^2 = 0.964 \quad (13)$$

- *Outer saddle position*

$$\mathrm{SCF_{OS}} = 3.134\beta^{0.796}\gamma^{1.003}\tau^{1.052}\zeta^{0.206}\theta^{1.661}(1 - 0.926\beta^{1.602} + 0.386\theta) \quad R^2 = 0.985 \quad (14)$$

- *Toe position*

$$\mathrm{SCF_{T}} = 1.291\beta^{0.030}\gamma^{0.572}\tau^{0.881}\zeta^{-0.075}\theta^{0.733}(1 - 0.688\beta^{0.988}) \quad R^2 = 0.920 \quad (15)$$

Values obtained for R^2, indicating the accuracy of the fit, are considered to be acceptable regarding the complex nature of the problem. The validity ranges of dimensionless geometrical parameters for the developed equations have been given in Eq. (11). It should be noted that, no design equation was developed for the heel position. The reason has been discussed in Sect. 4.3.

In Fig. 13, the SCF values predicted by proposed equations are compared with the SCF values extracted from FE analyses. It can be seen that there is a good agreement between the results of proposed equations and numerically computed values.

The UK Department of Energy (DoE) (1983) recommends the following assessment criteria regarding the applicability of the parametric equations (P/R stands for the ratio of the *predicted* SCF from a given equation to the *recorded* SCF from test or analysis):

- For a given dataset, if % SCF values under-predicting $\leq$ 25%, i.e., [%$P/R < 1.0$] $\leq$ 25%, and if % SCFs considerably under-predicting $\leq$ 5%, i.e., [%$P/R < 0.8$] $\leq$ 5%, then accept the equation. If, in addition, the percentage SCF values considerably over-predicting $\leq$ 50%, i.e. [%$P/R > 1.5$] $\geq$ 50%, then the equation is regarded as generally conservative.
- If the acceptance criteria is nearly met i.e., 25% < [%$P/R < 1.0$] $\leq$ 30%, and/or 5% < [%$P/R < 0.8$] $\leq$ 7.5%, then the equation is regarded as borderline and engineering judgment must be used to determine acceptance or rejection.
- Otherwise reject the equation as it is too optimistic.

In view of the fact that for a mean fit equation, there is always a large percentage of under-prediction, the requirement for joint under-prediction, i.e., $P/R < 1.0$, can be completely removed in the assessment of parametric equations (Bomel Consulting Engineers 1994). Assessment results according to the UK DoE (1983) criteria are presented in Table 5 showing that all the equations derived in the present research satisfy the criteria recommended by the UK Department of Energy.

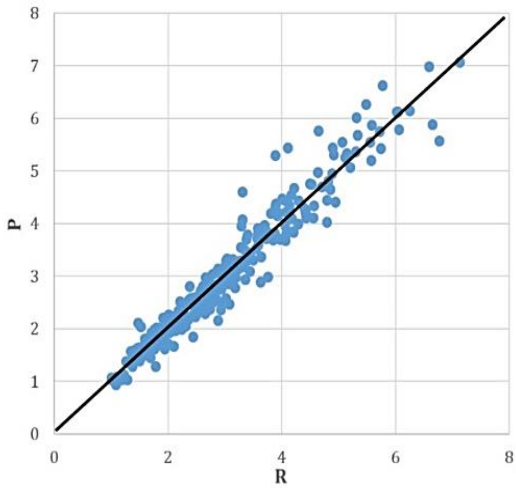

Fig. 13 Comparison of 243 SCF values calculated by the proposed equation for the toe position (Eq. (15)) with the corresponding SCF values extracted from the FE analysis (P: SCF value predicted by the equation, R: SCF value recorded from FE analysis)

Table 5 Results of SCF equations assessment according to the UK DoE (1983) acceptance criteria

Proposed equation	Conditions		Decision
	$\%P/R < 0.8$	$\%P/R > 1.5$	
Eq. (13)	1.2% < 5% OK.	16.8% < 50% OK.	Accept
Eq. (14)	0% < 5% OK.	15% < 50% OK.	Accept
Eq. (15)	2.1% < 5 % OK.	0% < 50% OK.	Accept

6. Conclusions

Results of stress analyses performed on 243 FE models verified against available experimental data were used to investigate the effects of geometrical parameters on the SCF values at the inner saddle, outer saddle, toe, and heel positions in multi-planar tubular KK-joints, also called two-planar K-joints or DK-joints, under axial loading. A set of SCF parametric equations was also developed for the fatigue design.

The increase of the parameters τ, γ, and θ leads to the increase of the SCFs at the inner saddle, outer saddle, toe, and heel positions. However, the increase of the β generally results in the decrease of the SCF values at these positions. The increase of the ζ generally leads to the decrease of the SCF at the inner saddle position; but it does not have a considerable effect on the SCF values at the other positions. The SCFs at the outer saddle and heel positions are the biggest and smallest values, respectively. High coefficients of determination and the satisfaction of acceptance criteria recommended by the UK DoE guarantee the accuracy of three parametric equations proposed in the present paper. Hence, the developed equations can reliably be used for the fatigue analysis and design of multi-planar tubular KK-joints subjected to axial loading.

Acknowledgments

Useful comments of anonymous reviewers on draft version of this paper are highly appreciated.

References

Ahmadi, H. and Ghaffari, A. (2015), "Probabilistic analysis of stress intensity factor (SIF) and degree of bending (DoB) in axially loaded tubular K-joints of offshore structures", *Lat. Am. J. Solids Struct.*, **12**(11), 202-2044. https://doi.org/10.1590/1679-78251698.

Ahmadi, H. and Imani, H. (2022), "SCFs in offshore two-planar tubular TT-joints reinforced with internal ring stiffeners", *Ocean Syst. Eng.*, **12**(1), 1-22. https://doi.org/10.12989/ose.2022.12.1.001.

Ahmadi, H. and Kouhi, A. (2020), "Stress concentration factors of multi-planar tubular XT-joints subjected to out-of-plane bending moments", *Appl. Ocean Res.*, **96**, 102058. https://doi.org/10.1016/j.apor.2020.102058.

Ahmadi, H., Lotfollahi-Yaghin, M.A. and Aminfar, M.H. (2011a), "Distribution of weld toe stress concentration factors on the central brace in two-planar CHS DKT-connections of steel offshore structures", *Thin-Wall. Struct.*, **49**, 1225-1236. https://doi.org/10.1016/j.tws.2011.06.001.

Ahmadi, H., Lotfollahi-Yaghin, M.A. and Aminfar, M.H. (2011b), "Effect of stress concentration factors on the structural integrity assessment of multi-planar offshore tubular DKT-joints based on the fracture mechanics fatigue reliability approach", *Ocean Eng.*, **38**, 1883-1893. https://doi.org/10.1016/j.oceaneng.2011.08.004.

Ahmadi, H., Lotfollahi-Yaghin, M.A. and Aminfar, M.H. (2011c), "Geometrical effect on SCF distribution in uni-planar tubular DKT-joints under axial loads", *J. Constr. Steel Res.*, **67**(8), 1282-1291. https://doi.org/10.1016/j.jcsr.2011.03.011.

Ahmadi, H., Lotfollahi-Yaghin, M.A. and Aminfar, M.H. (2012a), "The development of fatigue design formulas for the outer brace SCFs in offshore three-planar tubular KT-joints", *Thin-Wall. Struct.*, **58**, 67-78. https://doi.org/10.1016/j.tws.2012.04.011.

Ahmadi, H., Lotfollahi-Yaghin, M.A., Shao, Y.B. and Aminfar, M.H. (2012b), "Parametric study and formulation of outer-brace geometric stress concentration factors in internally ring-stiffened tubular KT-joints of offshore structures", *Appl. Ocean Res.*, **38**, 74-91. https://doi.org/10.1016/j.apor.2012.07.004.

Ahmadi, H., Lotfollahi-Yaghin, M.A. and Shao, Y.B. (2013), "Chord-side SCF distribution of central brace in internally ring-stiffened tubular KT-joints: A geometrically parametric study", *Thin-Wall. Struct.*, **70**, 93-105. https://doi.org/10.1016/j.tws.2013.04.011.

Ahmadi, H. and Lotfollahi-Yaghin, M.A. (2012a), "A probability distribution model for stress concentration factors in multi-planar tubular DKT-joints of steel offshore structures", *Appl. Ocean Res.*, **34**, 21-32. https://doi.org/10.1016/j.apor.2011.11.002.

Ahmadi, H. and Lotfollahi-Yaghin, M.A. (2013), "Effect of SCFs on S–N based fatigue reliability of multi-planar tubular DKT-joints of offshore jacket-type structures", *Ships Offshore Struct.*, **8**, 55-72. https://doi.org/10.1080/17445302.2011.627750.

Ahmadi, H. and Lotfollahi-Yaghin, M.A. (2012b), "Geometrically parametric study of central brace SCFs in offshore three-planar tubular KT-joints", *J. Constr. Steel Res.*, **71**, 149-161. https://doi.org/10.1016/j.jcsr.2011.10.024.

Ahmadi, H. and Lotfollahi-Yaghin, M.A. (2015), "Stress concentration due to in-plane bending (IPB) loads in ring-stiffened tubular KT-joints of offshore structures: Parametric study and design formulation", *Appl. Ocean Res.*, **51**, 54-66. https://doi.org/10.1016/j.apor.2015.02.009.

Ahmadi, H. and Mousavi Nejad Benam, M.A. (2017), "Probabilistic analysis of SCFs in unstiffened gap tubular KT-joints of jacket structures under the OPB moment loads", *Adv. Struct. Eng.*, **20**, 595-615. https://doi.org/10.1177%2F1369433216658487.

Ahmadi, H. and Zavvar, E. (2015), "Stress concentration factors induced by out-of-plane bending loads in ring-stiffened tubular KT-joints of jacket structures", *Thin-Wall. Struct.*, **91**, 82-95. https://doi.org/10.1016/j.tws.2015.02.011.

Ahmadi, H. and Zavvar, E. (2016), "The effect of multi-planarity on the SCFs in offshore tubular KT-joints subjected to in-plane and out-of-plane bending loads", *Thin-Wall. Struct.*, **106**, 148-165. https://doi.org/10.1016/j.tws.2016.04.020.

Ahmadi, H. (2016), "A probability distribution model for SCFs in internally ring-stiffened tubular KT-joints of offshore structures subjected to out-of-plane bending loads", *Ocean Eng.*, **116**, 184-199. https://doi.org/10.1016/j.oceaneng.2016.02.037.

Ahmadi, H., Mohammadi, A.H., Yeganeh, A. and Zavvar, E. (2016), "Probabilistic analysis of stress concentration factors in tubular KT-joints reinforced with internal ring stiffeners under in-plane bending loads", *Thin-Wall. Struct.*, **99**, 58-75. https://doi.org/10.1016/j.tws.2015.11.010.

Ahmadi, H., Mohammadi, A.H. and Yeganeh, A. (2015), "Probability density functions of SCFs in internally ring-stiffened tubular KT-joints of offshore structures subjected to axial load", *Thin-Wall. Struct.*, **94**, 485-499. https://doi.org/10.1016/j.tws.2015.05.012.

American Petroleum Institute (API) (2007), Recommended practice for planning, designing and constructing fixed offshore platforms: Working stress design: RP 2A-WSD. 21st Ed., Errata and Supplement 3, Washington DC, US.

American Welding Society (AWS) (2002), Structural welding code: AWS D 1.1. Miami (FL), US.

Asgarian, B., Mokarram, V. and Alanjari, P. (2014), "Local joint flexibility equations for Y-T and K-type tubular joints", *Ocean Syst. Eng.*, **4**(2), 151-167. httpd://doi.org/10.12989/ose.2014.4.2.151.

Bomel Consulting Engineers (1994), "Assessment of SCF equations using Shell/KSEPL finite element data", C5970R02.01 REV C, Bomel Consulting Engineers.

Cao, J.J., Yang, G.J. and Packer, J.A. (1997), "FE mesh generation for circular tubular joints with or without cracks", *Proceedings of the 7th International Offshore and Polar Engineering Con*ference, Honolulu (HI), US.

Chang, E. and Dover, W.D. (1999a), "Parametric equations to predict stress distributions along the intersection of tubular X and DT-joints", *Int. J. Fatigue*, **21**, 619-635. https://doi.org/10.1016/S0142-1123(99)00018-3.

Chang, E. and Dover, W.D. (1999b), "Prediction of stress distributions along the intersection of tubular Y and T-joints", *Int. J. Fatigue*, **21**, 361-381. https://doi.org/10.1016/S0142-1123(98)00083-8.

Chang, E. and Dover, W.D. (1996), "Stress concentration factor parametric equations for tubular X and DT joints", *Int. J. Fatigue*, **18**(6), 363-387. https://doi.org/10.1016/0142-1123(96)00017-5.

Chiew, S.P., Soh, C.K. and Wu, N.W. (1999), "Experimental and numerical stress analyses of tubular XT-joint", *J. Struct. Eng.*,**125**, 1239-1248. https://doi.org/10.1061/(ASCE)0733-9445(1999)125:11(1239).

Chiew, S.P., Soh, C.K. and Wu, N.W. (2000), "General SCF design equations for steel multiplanar tubular XX-joints", *Int. J. Fatigue*, **22**, 283-293. https://doi.org/10.1016/S0142-1123(99)00130-9.

Efthymiou, M. and Durkin, S. (1985), "Stress concentrations in T/Y and gap/overlap K-joints", *Proceedings of the Conference on Behavior of Offshore Structures*, Delft, the Netherlands.

Efthymiou, M. (1988), "Development of SCF formulae and generalized influence functions for use in fatigue analysis", *OTJ 88*, Surrey, UK.

Gao, F., Shao, Y.B. and Gho, W.M. (2007), "Stress and strain concentration factors of completely overlapped tubular joints under lap brace IPB load", *J. Constr. Steel Res.*, **63**, 305-316. https://doi.org/10.1016/j.jcsr.2006.05.007.

Gao, F. (2006), "Stress and strain concentrations of completely overlapped tubular joints under lap brace OPB load", *Thin-Wall. Struct.*, **44**, 861-871, https://doi.org/10.1016/j.tws.2006.08.017.

Gaspar, B., Garbatov, Y. and Guedes Soares, C. (2011), "Effect of weld shape imperfections on the structural hot-spot stress distribution", *Ships Offshore Struct.*, **6**(1-2), 145-159. https://doi.org/10.1080/17445302.2010.497052.

Gho, W.M. and Gao, F. (2004), "Parametric equations for stress concentration factors in completely overlapped tubular K(N)-joints", *J. Constr. Steel Res.*, **60**, 1761-1782. https://doi.org/10.1016/j.jcsr.2004.05.003.

Hellier, A.K., Connolly, M. and Dover, W.D. (1990), "Stress concentration factors for tubular Y and T-joints", *Int. J. Fatigue*, **12**, 13-23. https://doi.org/10.1016/0142-1123(90)90338-F.
Hoon, K.H., Wong, L.K. and Soh, A.K. (2001), "Experimental investigation of a doubler-plate reinforced tubular T-joint subjected to combined loadings", *J. Constr. Steel Res.*, **57**, 1015-1039. https://doi.org/10.1016/S0143-974X(01)00023-2.
IIW-XV-E (1999), Recommended fatigue design procedure for welded hollow section joints, IIW Docs, XV-1035-99/XIII-1804-99. International Institute of Welding, France.
Karamanos, S.A., Romeijn, A. and Wardenier, J. (2002), "SCF equations in multi-planar welded tubular DT-joints including bending effects", *Mar. Struct.*, **15**, 157-173, https://doi.org/10.1016/S0951-8339(01)00020-X.
Karamanos, S.A., Romeijn, A. and Wardenier, J. (1999), "Stress concentrations in multi-planar welded CHS XX-connections", *J. Constr. Steel Res.*, **50**, 259-282.https://doi.org/10.1016/S0143-974X(98)00244-2.
Karamanos, S.A., Romeijn, A. and Wardenier, J. (2000), "Stress concentrations in tubular gap K-joints: mechanics and fatigue design", *Eng. Struct.*, **22**, 4-14, https://doi.org/10.1016/S0141-0296(98)00062-5.
Kuang, J.G., Potvin, A.B. and Leick, R.D. (1975), "Stress concentration in tubular joints", *Proceedings of the Offshore Technology Conference*, Paper OTC 2205, Houston (TX), US.
Lee, M.K. and Wilmshurst, S.R. (1995), "Numerical modeling of CHS joints with multiplanar double-K configuration", *J. Constr. Steel Res.*, **32**, 281-301. https://doi.org/10.1016/0143-974X(95)93899-F.
Lee, M.M.K. (1999), "Strength, stress and fracture analyses of offshore tubular joints using finite elements", *J. Constr. Steel Res.*, **51**, 265-286. https://doi.org/10.1016/S0143-974X(99)00025-5.
Liu, G., Zhao, X. and Huang, Y. (2015), "Prediction of stress distribution along the intersection of tubular T-joints by a novel structural stress approach", *Int. J. Fatigue*, **80**, 216-230. https://doi.org/10.1016/j.ijfatigue.2015.05.021.
Lotfollahi-Yaghin, M.A. and Ahmadi, H. (2010), "Effect of geometrical parameters on SCF distribution along the weld toe of tubular KT-joints under balanced axial loads", *Int. J. Fatigue*, **32**, 703-719, https://doi.org/10.1016/j.ijfatigue.2009.10.008.
Lotfollahi-Yaghin, M.A. and Ahmadi, H. (2011), "Geometric stress distribution along the weld toe of the outer brace in two-planar tubular DKT-joints: parametric study and deriving the SCF design equations", *Mar. Struct.*, **24**, 239-260. https://doi.org/10.1016/j.marstruc.2011.02.005.
Morgan, M.R. and Lee, M.M.K. (1998a), "Parametric equations for distributions of stress concentration factors in tubular K-joints under out-of-plane moment loading", *Int. J. Fatigue*, **20**, 449-461. https://doi.org/10.1016/S0142-1123(98)00011-5.
Morgan, M.R. and Lee, M.M.K. (1998b), "Prediction of stress concentrations and degrees of bending in axially loaded tubular K-joints", *J. Constr. Steel Res.*, **45**(1), 67-97. https://doi.org/10.1016/S0143-974X(97)00059-X.
Myers, P.T., Brennan, F.P. and Dover, W.D. (2001), "The effect of rack/rib plate on the stress concentration factors in jack-up chords", *Mar. Struct.*, **14**, 485-505. https://doi.org/10.1016/S0951-8339(00)00051-4.
N'Diaye, A., Hariri, S., Pluvinage, G. and Azari, Z. (2007), "Stress concentration factor analysis for notched welded tubular T-joints", *Int. J. Fatigue*, **29**, 1554-1570. https://doi.org/10.1016/j.ijfatigue.2006.10.030.
Nassiraei, H. and Chavoshi, H.R. (2024), "Collar plate effect on local joint flexibility of tubular K-joints under IPB moments: Parametric study and predictive equations", *Mar. Struct.*, **98**, 103676. https://doi.org/10.1016/j.marstruc.2024.103676.
Nassiraei, H. (2022), "Geometrical effects on the LJF of tubular T/Y-joints with doubler plate in offshore wind turbines", *Ships Offshore Struct.*, **17**, 481-491. https://doi.org/10.1080/17445302.2020.1835051.
Nassiraei, H. (2020), "Local joint flexibility of CHS T/Y-connections strengthened with collar plate under in-plane bending load: Parametric study of geometrical effects and design formulation", *Ocean Eng.*, **202**, 107054. https://doi.org/10.1016/j.oceaneng.2020.107054.
Nassiraei, H. (2019a), "Local joint flexibility of CHS X-joints reinforced with collar plates in jacket structures subjected to axial load", *Appl. Ocean Res.*, **93**, 101961. https://doi.org/10.1016/j.apor.2019.101961.
Nassiraei, H. (2024a), "Probabilistic analysis of strength in retrofitted X-joints under tensile loading and fire conditions", *Building*, **14**, 2105. https://doi.org/10.3390/buildings14072105.

Nassiraei, H. (2024b), “Probability distribution functions for the ultimate strength of X-joints with collar plates in compressive load at room and fire conditions”, *Struct.*, **59**, 105703. https://doi.org/10.1016/j.istruc.2023.105703.

Nassiraei, H. (2023), “Probability distribution models for the ultimate strength of tubular T/Y-joints reinforced with collar plates at room and different fire conditions”, *Ocean Eng.*, **270**, 113557. https://doi.org/10.1016/j.oceaneng.2022.113557.

Nassiraei, H. and Rezadoost, P. (2021a), “Parametric study and formula for SCFs of FRP-strengthened CHS T/Y-joints under out-of-plane bending load”, *Ocean Eng.*, **221**, 108313. https://doi.org/10.1016/j.oceaneng.2020.108313.

Nassiraei, H. and Rezadoost, P. (2021b), “Stress concentration factors in tubular T/Y-connections reinforced with FRP under in-plane bending load”, *Mar. Struct.*, **76**, 102871. https://doi.org/10.1016/j.marstruc.2020.102871.

Nassiraei, H. and Rezadoost, P. (2020), “Stress concentration factors in tubular T/Y-joints strengthened with FRP subjected to compressive load in offshore structures”, *Int. J. Fatigue*, **140**, 105719. https://doi.org/10.1016/j.ijfatigue.2020.105719.

Nassiraei, H. (2019b), “Static strength of tubular T/Y-joints reinforced with collar plates at fire induced elevated temperature”, *Mar. Struct.*, **67**, 102635. https://doi.org/10.1016/j.marstruc.2019.102635.

Nassiraei, H. and Yara, A. (2022a), “Local joint flexibility of tubular K-joints reinforced with external plates under IPB loads”, *Mar. Struct.*, **84**, 103199. https://doi.org/10.1016/j.marstruc.2022.103199.

Nassiraei, H. and Yara, A. (2023), “Local joint flexibility of tubular K-joints reinforced with external plates under out of plane bending moments”, *Ships Offshore Struct.*, **18**, 1688-1700. https://doi.org/10.1080/17445302.2022.2140508.

Nassiraei, H. and Yara, A. (2022b), “Numerical analysis of local joint flexibility of K-joints with external plates under axial loads in offshore tubular structures”, *J. Mar. Sci. Appl.*, **21**, 134-144. https://doi.org/10.1007/s11804-022-00302-w.

Nwosu, D.I., Swamidas, A.S.J. and Munaswamy, K. (1995), “Numerical stress analysis of internal ring-stiffened tubular T-joints”, *J. Offshore Mech. Arct.*, **117**, 113-125. https://doi.org/10.1115/1.2827061.

Prashob, P.S., Shashikala, A.P. and Somasundaran, T.P. (2018), “Effect of FRP parameters in strengthening the tubular joint for offshore structures”, *Ocean Syst. Eng.*, **8**(4), 409-426. https://doi.org/10.12989/ose.2018.8.4.409.

Shao, Y.B., Du, Z.F. and Lie, S.T. (2009), “Prediction of hot spot stress distribution for tubular K-joints under basic loadings”, *J. Constr. Steel Res.*, **65**, 2011-2026. https://doi.org/10.1016/j.jcsr.2009.05.004.

Shao, Y.B. (2004a), “Fatigue behaviour of uni-planar CHS gap K-joints under axial and in-plane bending loads”, Ph.D. Dissertation, School of Civil & Environmental Engineering, Nanyang Technological University, Singapore.

Shao, Y.B. (2007), “Geometrical effect on the stress distribution along weld toe for tubular T- and K-joints under axial loading”, *J. Constr. Steel Res.*, **63**, 1351-1360. https://doi.org/10.1016/j.jcsr.2006.12.005.

Shao, Y.B. (2004b), “Proposed equations of stress concentration factor (SCF) for gap tubular K-joints subjected to bending load”, *Int. J. Space Struct.*, **19**, 137-147. https://doi.org/10.1260%2F0266351042886667.

Smedley, P. and Fisher, P. (1991), “Stress concentration factors for simple tubular joints”, *Proceedings of the International Offshore and Polar Engineering Conference (ISOPE)*, Edinburgh.

UK Department of Energy (DoE) (1983), “Background notes to the fatigue guidance of offshore tubular joints”, UK DoE, London, UK.

UK Health and Safety Executive (HSE) (1997), “OTH 354: Stress concentration factors for simple tubular joints − assessment of existing and development of new parametric formulae”, UK HSE, London, UK.

Underwater Engineering Group (UEG) (1985), “Design of tubular joints for offshore structures”, UEG/CIRIA, London (UK).

Wingerde, A.M., Packer, J.A. and Wardenier, J. (2001), “Simplified SCF formulae and graphs for CHS and RHS K- and KK-connections”, *J. Constr. Steel Res.*, **57**, 221-252. https://doi.org/10.1016/S0143-974X(00)00015-8.

Woghiren, C.O. and Brennan, F.P. (2009), "Weld toe stress concentrations in multi planar stiffened tubular KK Joints", *Int. J. Fatigue*, **31**, 164-172. https://doi.org/10.1016/j.ijfatigue.2008.03.039.

Xu, F., Chen, J. and Jin, W. (2015), "Experimental investigation of SCF distribution for thin-walled concrete-filled CHS joints under axial tension loading", *Thin-Wall. Struct.*, **93**, 149-157. https://doi.org/10.1016/j.tws.2015.03.019.

Yang, J., Chen, Y. and Hu, K. (2015), "Stress concentration factors of negative large eccentricity tubular N-joints under axial compressive loading in vertical brace", *Thin-Wall. Struct.*, **96**, 359-371. https://doi.org/10.1016/j.tws.2015.08.027.

Zhao, X.L., Herion, S., Packer, J.A., Puthli, R., Sedlacek, G. and Wardenier, J. (2000), "Design guide for circular and rectangular hollow section joints under fatigue loading", CIDECT Publication, No. 8, TUV Verlag, Germany.

MK

Nomenclature

d	Outer diameter of the brace
D	Outer diameter of the chord
DoE	Department of Energy
FE	Finite elements
g	Gap
HSS	Hot-spot stress
IPB	In-plane bending
IS	Inner saddle
L	Chord length
OPB	Out-of-plane bending
OS	Outer saddle
R^2	Coefficient of determination
SCF	Stress concentration factor
t	Brace wall thickness
T	Toe
T	Chord wall thickness
$X_{\perp}$	Direction perpendicular to the weld toe
α	Chord slenderness ratio (=$2L/D$)
α_B	Brace slenderness ratio (=$2l/d$)
β	Brace-to-chord diameter ratio (=d/D)
γ	Chord wall slenderness ratio (=$D/2T$)
ψ	Dihedral angle
$\sigma_{\perp W}$	Extrapolated geometric stress at the weld toe
σ_n	Nominal stress
τ	Brace-to-chord thickness ratio (=t/T)
θ	Brace inclination angle
ζ	Relative gap (=g/D)